THE JOURNAL OF BIOLOGICAL CHEMISTRY
Vol. 278, No. 31, Issue of August 1, pp. 29079–29085, 2003
Printed in U.S.A.

Evidence for Intersubunit Interactions between S4 and S5 Transmembrane Segments of the Shaker Potassium Channel*

Received for publication, February 25, 2003, and in revised form, May 1, 2003
Published, JBC Papers in Press, May 21, 2003, DOI 10.1074/jbc.M301991200/6493

Edward J. Neale, David J. S. Elliott, Malcolm Hunter, and Asipu Sivaprasadarao‡

From the School of Biomedical Sciences, Leeds University, Leeds LS2 9JT, United Kingdom

Voltage-gated potassium channels are transmembrane proteins made up of four subunits, each comprising six transmembrane (S1-S6) segments. S1-S4 form the voltage-sensing domain and S5-S6 the pore domain with its central pore. The sensor domain detects membrane depolarization and transmits the signal to the activation gates situated in the pore domain, thereby leading to channel opening. An understanding of the mechanism by which the sensor communicates the signal to the pore requires knowledge of the structure of the interface between the voltage-sensing and pore domains. Toward this end, we have introduced single cysteine mutations into the extracellular end of S4 (positions 356 and 357) in conjunction with a cysteine in S5 (position 418) of the Shaker channel and expressed the mutants in *Xenopus* oocytes. We then examined the propensity of each pair of engineered cysteines to form a metal bridge or a disulfide bridge, respectively, by examining the effect of Cd^{2+} ions and copper phenanthroline on the K^+ conductance of a whole oocyte. Both reagents reduced currents through the S357C,E418C double mutant channel, presumably by restricting the movements necessary for coupling the voltage-sensing function to pore opening. This inhibitory effect was seen in the closed state of the channel and with heteromers composed of S357C and E418C single mutant subunits; no effect was seen with homomers of any of the single mutant channels. These data indicate that the extracellular end of S4 lies in close proximity to the extracellular end of the S5 of the neighboring subunit in closed channels.

Voltage-gated potassium (K_v)[1] channels are made up of four identical or homologous subunits that assemble to form a central pore domain and four voltage-sensing domains (1–4). The pore and the voltage-sensing domains are functionally coupled such that when the membrane is depolarized the subsequent movement of the voltage-sensing domains leads to channel opening (1–5). All channels contain activation gates that open to let K^+ ions flow through the aqueous pore located in the center of the pore domain. Some channel pores contain inactivation gates that close during depolarization, resulting in the termination of ion flux, although the activation gates may remain open (2, 3, 6).

Each subunit of the channel consists of six transmembrane segments (S1-S6). Of these, S5 to S6 and the connecting P-loop make up the pore domain. The remaining segments (S1-S4) comprise the voltage-sensing domain (Fig. 1). Although the x-ray structure is not known for any member of the K_v channel family, current evidence suggests that the pore domain of the channel is homologous to bacterial potassium channels (7–9). The activation gate is formed by the crossing of "inner helices" at the intracellular end of the pore. The mechanism by which these gates open has become clear from the structures of KcsA (7, 8) and MthK (9) in the closed and open states, respectively. However, site-directed cysteine accessibility studies suggested that there may be some differences in the way the gates move in K_v channels (10, 11); these differences may have been evolved to facilitate coupling of activation gates to the voltage sensor.

The inactivation gate, which confers C-type inactivation in K_v channels, appears to be located at the extracellular end of the pore above the selectivity filter (6, 12, 13). During depolarization, residues contributing to the inactivation gate move to pinch shut the pore, thereby terminating ion flux. Like the activation gates, inactivation gates are also coupled to the voltage sensor (6, 13–15).

The signal that triggers the movement of gates in the pore domain originates in the voltage-sensing domain. Cysteine and histidine scanning mutagenesis experiments revealed that during depolarization, the positively charged S4 segment, which is thought to be the main component of the voltage sensor, moves out of the membrane field, exposing a number of membrane-embedded S4 residues to the extracellular solvent (16–21). This is accompanied by the entry of several of the cytoplasmically accessible S4 residues into the membrane bilayer (16, 17). By measuring changes in fluorescence of the probes attached to S4, Bezanilla and coworkers (22) and Isacoff and coworkers (23) showed that S4 rotates during depolarization. In addition, more recent studies demonstrated that S4 might move laterally (24).

Although the movements of S4 and the gates are known to some extent, the mechanism whereby the movements in the voltage sensor are coupled to the motion of pore gates is not known. Structure perturbation studies have revealed residues on the pore domain that appear to interact with the voltage-sensing domain, but it is not clear which residues of the voltage sensor are involved in the interaction (25–27). Other studies showed that the extracellular end of S4 moves toward the periphery of the pore domain during depolarization, indicating that the voltage signal may be communicated to the gates of the pore through physical interaction (28, 29). However, the details of residue-residue contacts between S4 and the pore domain and how the contacts change during channel gating are still lacking.

In the absence of a three-dimensional structure, the identity

* This work was supported by the Wellcome Trust. The costs of publication of this article were defrayed in part by the payment of page charges. This article must therefore be hereby marked "*advertisement*" in accordance with 18 U.S.C. Section 1734 solely to indicate this fact.

‡ To whom correspondence should be addressed. Tel.: 44-0113-3434326; Fax: 44-0-113-3434228; E-mail: a.sivaprasadarao@leeds.ac.uk.

[1] The abbreviations used are: K_v, voltage-gated potassium; S, segment; DMPS, 2,3-dimercaptopropanesulfonate; BMS, bis(2-mercaptoethylsulfone); TCEP, tris(2-carboxyethyl)phosphine hydrochloride.

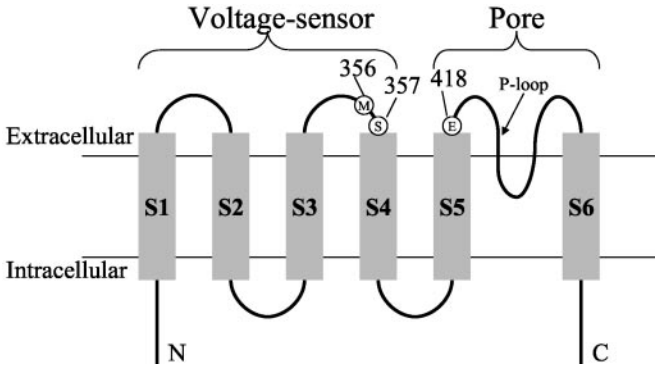

FIG. 1. **Putative transmembrane topology of the Shaker K channel subunit.** The putative positions of residues (Met-356, Ser-357, and Glu-418) mutated to cysteine are shown in *circles*. Transmembrane segments (S1-S6) are shown as *rectangles*.

of residues closely placed in the three-dimensional structure of a protein can be determined by the engineered metal (12, 30–33) and disulfide (12, 24, 31, 34, 35) bridge approaches. Such approaches are not only capable of revealing the identity of closely placed residues but, more importantly, report changes in their relative positions during function, thereby providing important insight into the molecular rearrangements underlying protein function. The power of these approaches has been illustrated with receptors (34, 36) and channels, including potassium channels (12, 13, 24, 30–33).

In this study, we examined whether S4 residues of the Shaker K channel are close enough to physically interact with its pore domain. For this, we have investigated the proximity of Met-356 and Ser-357 of S4 to Glu-418 of the pore domain (Fig. 1). The reasons for this choice of residues are as follows: site-directed cysteine accessibility method studies showed that Met-356 and Ser-357 are located outside the outer membrane interface (16–19). According to homology modeling based on the KcsA structure, Glu-418 is also located just outside the membrane border (top of S5) (37). Structure perturbing functional studies revealed that Glu-418 is located among the cluster of gating-sensitive residues of the pore domain, that is, the region via which the voltage sensor transmits its signal (25, 38). These observations suggest that Glu-418 is the likely residue with which the top of S4 interacts. To test this hypothesis, we have substituted cysteines into the Shaker K channel (Fig. 1) and investigated whether the cysteine at 418 can be cross-linked to S4 cysteines with a Cd^{2+} ion or a disulfide bridge. Our data show that (i) the cysteine at 418 forms a Cd^{2+} metal bridge as well as a disulfide bridge with the cysteine at 357, (ii) both the metal bridge and disulfide bond formation occur in the closed state of the channel, and (iii) the metal bridge is formed between Cys-357 and -418 of neighboring subunits. Taken together, we have identified a site of physical interaction between S4 and the pore domain that may play a critical role in transmission of the voltage signal to the pore domain.

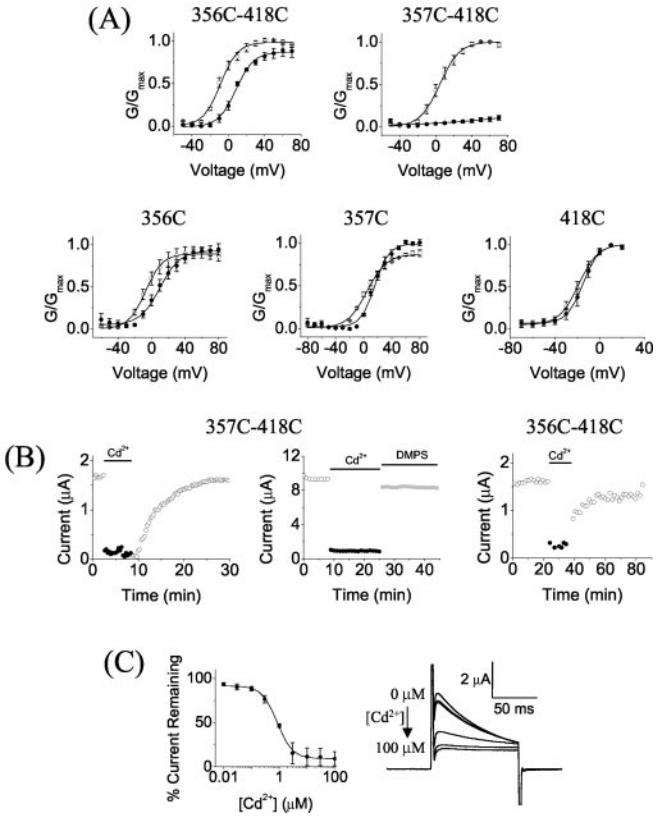

FIG. 2. **Effects of Cd^{2+} ions on cysteine mutants of the Shaker K channel.** *A*, normalized conductance-voltage curves for the indicated cysteine mutant channels, recorded in the absence (○) and presence (●) of Cd^{2+} (100 μM) as described under "Experimental Procedures." Data points (mean ± S.E.; $n \geq 3$) were fitted to Boltzmann function. *B*, representative data for the time course of the effect of Cd^{2+} on peak currents from the indicated double mutant channels recorded during depolarizing steps to +40 mV (S357C,E418C) or 0 mV (M356C,E418C). Cd^{2+} (100 μM) and DMPS (0.1 mM) were applied over the period indicated by the *horizontal bars*. Current amplitudes recorded in the presence of these reagents are shown as *filled circles*. *C*, effect of increasing concentrations of Cd^{2+} on currents from S357C,E418C mutant channels. Data were fitted with a Hill equation, from which an EC_{50} of 0.8 ± 0.1 μM was calculated. Current traces corresponding to one set of data are shown on the *right* (from top to bottom: 0, 0.01, 0.1, 1, 10, and 100 μM Cd^{2+}).

EXPERIMENTAL PROCEDURES

Molecular Biology—Amino acid substitutions were introduced into the inactivation ball (residues 6–46)-removed Shaker potassium channel (39) by site-directed mutagenesis using the QuikChange method (Stratagene). cRNA transcripts were made from *Not*I-linearized plasmid (pEXO, a pSK Bluescript derivative containing the 5′- and 3′-untranslated regions of *Xenopus* globin cDNA) constructs containing the wild-type and mutant cDNA sequences using the T7 MEGAScript kit (Ambion). All methods are as previously described (24).

Electrophysiology—Oocytes were isolated from *Xenopus* laevis. The animals were anesthetized by immersion in 0.2% 3-aminobenzoic acid ethyl ester (Sigma) and killed by cervical dislocation. Ovarian lobes were surgically removed and digested with collagenase (1 mg/ml, Type 1A; Sigma) for 90 min. Dumont stage V or VI oocytes were selected and injected with 5–20 ng of cRNA. Oocytes were incubated at 18 °C in modified ND96 solution containing (mM): 96 NaCl, 2 KCl, 1 $MgSO_4$, 1.8 $CaCl_2$, 0.1 dithiothreitol, and 5 HEPES, pH 7.4, supplemented with penicillin (10 units ml^{-1}), gentamicin (50 μg ml^{-1}), and streptomycin (0.1 mg ml^{-1}). Whole cell currents were recorded between 1 and 3 days after injection using a two-electrode voltage clamp in Ringer's solution containing (mM): 115 NaCl, 2 KCl, 1.8 $CaCl_2$, 10 HEPES, pH 7.2. Microelectrodes were made from borosilicate glass, filled with 3 M KCl, and had resistances between 0.5 and 2.0 MΩ.

Current (*I*)-voltage (*V*) relationships were measured from oocytes by stepping to positive potentials in 10-mV increments from a holding potential of −80 mV; the steps were applied at 20-s intervals and lasted for 50–500 ms. Conductance (*G*) values were calculated from peak currents using the equation $G = I/(V-V_{rev})$, where V_{rev} is the reversal potential. The *G-V* data were fitted to the Boltzmann function, $G/G_{max} = 1/(1+\exp(V_{0.5}-V)/k)$, where $V_{0.5}$ is the midpoint of half-maximal current and k is the slope factor (= RT/zF, where R is the gas constant, T the absolute temperature, z the valence, and F the Faraday constant).

To measure the effect of modification reagents, control currents were first measured in Ringer's solution during repeated depolarizing steps given from a holding potential of −80 mV. The cells were then superfused with Cd^{2+} (0.01–100 μM) or the copper (II) phenanthroline reagent (Cu-Phe, 5 μM Cu^{2+}:15 μM phenanthroline), made up in Ringer's

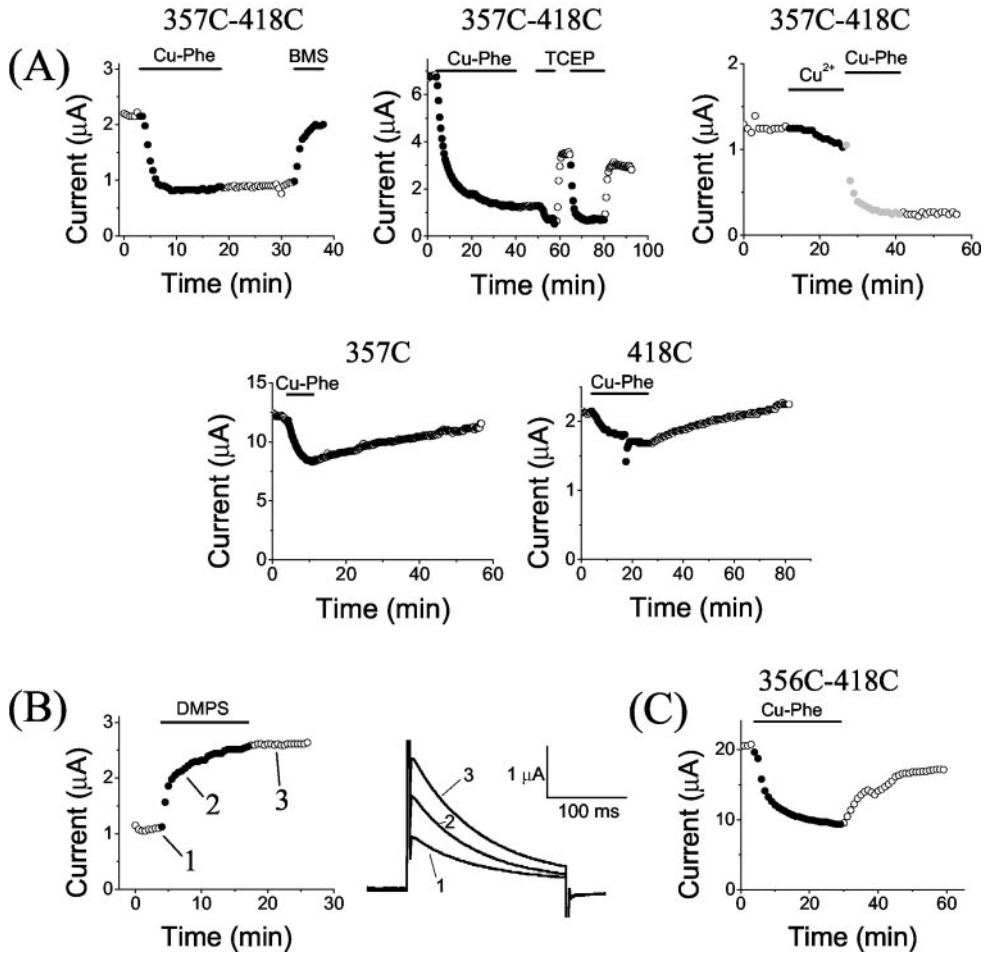

FIG. 3. **A disulfide bridge is formed between introduced cysteines in the S357C,E418C mutant channel.** *A* and *C*, representative traces for the effects of Cu-Phe on currents for the indicated mutants, recorded during depolarizing steps to 0 mV (S357C and E418C), +20 mV (M356C,E418C), or +40 mV (S357C,E418C). Cu-Phe (5 μM), Cu^{2+} (150 nM), DMPS (0.1 mM), BMS (0.1 mM), and TCEP (1 mM) were applied over the period indicated by the *horizontal bars*. Current amplitudes recorded in the presence of these reagents are shown as *filled circles*. *B*, disulfide bridge formation in S357C,E418C mutant channels by ambient oxygen. Representative time course of currents during the application of 0.1 mM DMPS (indicated by the *horizontal bar* and *filled circles*) and current traces corresponding to the time points, numbered *1–3*, are shown.

solution. Current recordings were continued until a steady-state effect was achieved. To examine the reversal of the effects, metal chelating/reducing agents (0.1 mM 2,3-dimercaptopropanesulfonate, DMPS; 0.1 mM bis(2-mercaptoethylsulfone), BMS; or 1.0 mM tris(2-carboxyethyl)-phosphine hydrochloride, TCEP) were perfused. To investigate the voltage dependence of the reagent effects, after measuring the control currents (as mentioned above) the cells were held at −80 mV for 30 s to allow recovery from any inactivation. Cd^{2+} was then applied for 4 min while holding at this potential before washing for 2 min and recommencing current measurements. All experiments were repeated at least three times ($n \geq 3$), and the data presented are either representative or mean ± S.E. Significance of any effects was calculated using a one-tailed Student's *t* test.

RESULTS

Cd^{2+} Abolishes K^+ Conduction Through the S357C,E418C Mutant Channel—To investigate whether the extracellular end of S4 is proximal to that of the pore domain, cysteines were substituted at positions 356 and 357 of S4 in conjunction with a cysteine at position 418 of the pore domain of the Shaker K channel (Fig. 1). The resultant mutant channels were expressed in *Xenopus* oocytes. The effect of extracellular application of submillimolar concentration (100 μM) of Cd^{2+} on properties of the channels was studied by the two-electrode voltage clamp technique. Fig. 2*A* shows that Cd^{2+} inhibits S357C,E418C double mutant channels at all potentials tested. The corresponding single mutants were either unaffected (E418C) or showed a small rightward shift (S357C, 10.8 ± 1.6 mV; $p < 0.05$) in the conductance-voltage (G–V) relationship. The profound effect of Cd^{2+} on the double, but not on the single, mutant channels suggests that Cd^{2+} might form a bridge between the cysteines at positions 357 and 418. The slow reversal of the effect (Fig. 2*B*; time constant for reversal, τ = 5.9 ± 2.4 min) with Ringer's solution is consistent with the strong binding of Cd^{2+} to the double mutant channel. As expected, the rate of reversal was faster (too fast to measure accurately) with DMPS, a reagent capable of chelating Cd^{2+} (Fig. 2*B*).

The M356C,E418C double mutations, on the other hand, caused no significant reduction in the maximal conductance of the channel but caused a rightward shift (15.9 ± 3.0 mV) in the G-V relationship. This effect of Cd^{2+} on this double mutant channel was found to be not significantly different from that of the M356C single mutant channel ($p > 0.05$). In addition, in this case, the effect (manifested as a reduction in current at 0 mV caused by the rightward shift in $V_{0.5}$) of Cd^{2+} can be readily washed off with Ringer's solution (Fig. 2*B*), indicating weak binding of Cd^{2+}. It therefore seems unlikely that Cd^{2+} forms a metal bridge between cysteines at positions 356 and 418.

Because the EC_{50} of the Cd^{2+} effect provides an indication of the number of residues to which the metal ion is coordinated (12, 30, 32, 33), we have examined the effect of Cd^{2+} concentration on currents through the S357C,E418C mutant channel.

Fig. 2*C* shows that Cd^{2+} reduces the amplitude of currents with an EC_{50} of 0.8 ± 0.1 μM. This value is consistent with the participation of at least two coordinating residues, possibly involving both the engineered cysteines.

Cysteines at Positions 357 and 418 Can Be Oxidized to Form Disulfide Bridges—Although the above data suggest that Cd^{2+} forms a metal bridge between Cys-357 and Cys-418, we cannot rule out the possibility that the combined mutations might have introduced subtle structural changes, thereby creating a Cd^{2+} binding site (for example, an allosteric site) not involving the engineered cysteines. It is known that Cd^{2+} can ligand to residues other than cysteine, including histidine, aspartic acid, glutamic acid, and methionine. In fact, there are a number of such residues in the extracellular portion of the channel protein that could contribute to the formation of such a Cd^{2+} binding site. In addition, Cd^{2+} caused a slowing of activation in the S357C single mutant. Because the slowing of activation overlaps the time course of C-type inactivation, it was difficult to resolve the Cd^{2+}-induced reduction in conductance from that resulting from changes in activation and inactivation kinetics. For these reasons, we have used the disulfide bridge approach, which involves induction of disulfide bonds between closely placed cysteine residues, using mild oxidizing agents such as copper (II) phenanthroline (Cu-Phe) (12, 13, 24, 31, 34).

Fig. 3*A* shows that the application of Cu-Phe to S357C,E418C caused rapid inhibition (τ = 2.5 ± 0.4 min) of currents; the extent of inhibition, however, varied from 65 to 80% between oocytes. The effect could not be washed off with Ringer's solution, indicating the irreversible nature of the modification. The corresponding single mutant channels, S357C and E418C, were also inhibited by Cu-Phe but only partially (≤30%); moreover, these effects could be completely washed off with Ringer's solution, indicating that the inhibition is more likely caused by the noncovalent binding of free Cu^{2+} ions present in the Cu-Phe reagent. The effect on the double mutant channel could be reversed with BMS, a disulfide reducing agent. Although other reducing agents, including dithiothreitol and DMPS, also reversed the effects, the reversal was only partial (data not shown). The ability of BMS to fully reverse the effect may be attributed to its higher accessibility (40).

The reversal of the Cu-Phe effect by the reducing agents is consistent with disulfide bond formation between Cys-357 and -418; however, we cannot completely rule out the possibility that Cu-Phe might have oxidized the cysteines to products other than disulfides, such as sulfonate derivatives (34). To eliminate this possibility, we used TCEP, a reagent specific for reducing the disulfide bonds (24, 41). Application of TCEP failed to reverse the inhibition caused by Cu-Phe (Fig. 3*A*). However, during the subsequent wash with Ringer's solution, over 50% of the inhibited current was recovered, indicating reduction of disulfide bond. Reapplication of TCEP caused inhibition of the recovered current, which could once again be reversed with a Ringer's wash (TCEP had a similar reversible inhibitory effect on the wild-type Shaker channel; data not shown). Thus these data provide further support to the argument that a disulfide bridge can be readily formed between Cys-357 and -418.

It is unlikely that the inhibition of S357C,E418C mutant channel by Cu-Phe is because of free Cu^{2+} ions present in the reagent; the concentration of uncomplexed Cu^{2+} ions would be expected to be too low (concentration of free Cu^{2+} in the reagent calculated using the stability constant 2×10^6 M^{-1} (42) is 1.5 nM) to cause a significant effect. Consistent with this expectation, application of a 100-fold excess of free Cu^{2+} had little effect on the currents, but a subsequent application of Cu-Phe resulted in rapid inhibition (Fig. 3*A*). To investigate whether disulfides are formed spontaneously in the double mutant channel, we next examined the effect of DMPS on channels from oocytes incubated in dithiothreitol-free medium. Fig. 3*B* shows that the application of DMPS caused over 100% increase in currents from an oocyte expressing the S357C,E418C double mutant channel; the extent of increase in current, however, varied from oocyte to oocyte. No such increase was observed with the corresponding single mutant channels (data not shown). As for the M356C,E418C double mutant channel, Cu-Phe caused over 50% inhibition of currents, but the effect was almost completely reversed with Ringer's wash (Fig. 3*C*), indicating that the engineered cysteines in this mutant channel are not close enough to undergo oxidation to disulfides. Taken together with the Cd^{2+} data (Fig. 2), we conclude that cysteines at positions 357 and 418, but not 356 and 418, are close to each other in the three-dimensional structure of the channel protein.

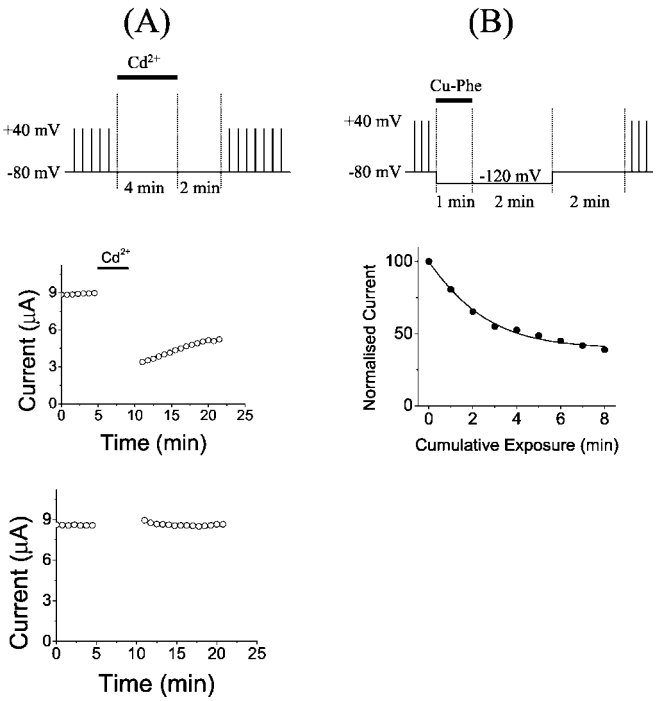

FIG. 4. **Voltage dependence of current inhibition in the S357C,E418C mutant channel.** *A*, effect of Cd^{2+} on S357C,E418C mutant channels while held at −80 mV. After establishing baseline responses with depolarizing steps to +40 mV from a holding potential of −80 mV, channels were held without pulsing for 4 min during which Cd^{2+} (100 μM) or Ringer's solution (control) were perfused; protocol shown at the *top*. Cd^{2+} was then washed off for 2 min, before pulsing was recommenced. Representative data obtained from a single oocyte are shown. *B*, voltage-dependent effect of Cu-Phe on S357C,E418C mutant channels during cumulative exposure to the reagent. After baseline recordings at +40 mV as in *panel A*, channels were held at −120 mV (●) for 1 min during which Cu-Phe (5 μM) was perfused. Cu-Phe was then washed off before measurement was recommenced. Protocol is shown at the *top*.

Cysteines at Positions 357 and 418 Lie Close to Each Other in the Closed State of the Channel—We next examined the voltage dependence of both Cd^{2+} and Cu-Phe effects on the S357C,E418C mutant channel. For this, we applied Cd^{2+} while holding the membrane potential of the oocyte at −80 mV. We then washed with Ringer's solution to prevent any Cd^{2+} binding during subsequent current measurements at +40 mV. Fig 4*A* shows over 60% current reduction during the first pulse after the 2-min washout, suggesting that Cd^{2+} forms a metal bridge in the closed state of the channel. No such inhibition was seen in the absence of Cd^{2+} perfusion. Because the effect of Cu-Phe, unlike that of Cd^{2+}, was fully resistant to Ringer's

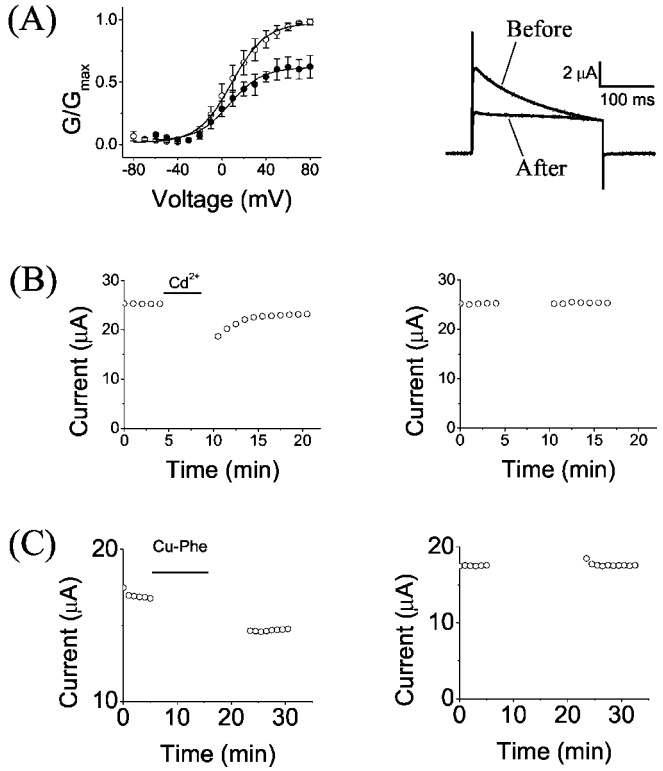

FIG. 5. **Current reduction in the S357C,E418C mutant channel is caused by an intersubunit cross-linking.** *A*, normalized conductance-voltage curves recorded in the absence (○) and presence (●) of Cd^{2+} (100 μM) from oocytes co-injected with a mixture (1:1 ratio) of cRNA for S357C and E418C single mutant channels as described in Fig. 2*A*. Representative current traces (recorded during +40 mV steps from a holding potential of −80 mV) before and after the application of Cd^{2+} are shown on the *right*. *B*, voltage dependence of Cd^{2+} effect on co-injected channels was measured as described in Fig. 4*A*. *C*, voltage dependence of Cu-Phe effect on co-injected channels, measured as described in Fig. 4*A*. The reagent was applied while holding the membrane potential at −120 mV. Cu-Phe was washed off, and currents were measured after a 4-min rest at −80 mV.

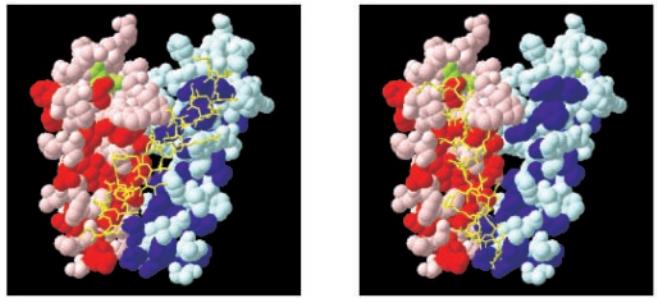

FIG. 6. **Potential orientation of S4 helices relative to the pore domain in the closed state of the Shaker channel.** The pore domain residues (392–480) of the Shaker subunits were mapped onto the KcSA x-ray structure and shown as a space-filled model; only two subunits are shown for sake of clarity. Residues highlighted in *red* on the *light pink* subunit and *blue* on the *light blue* subunit represent gating-sensitive amino acids that are thought to interact with the voltage-sensing domain, according to Li-Smerin *et al.* (25). Two possible orientations of S4 (shown in *yellow* as an α-helix) are shown to account for the present data and those of Li-Smerin *et al.* (25). In both models, S4 is positioned at an angle that crosses the intersubunit interface to allow (a) the top end (position 357) of S4 to lie close to position 418 (*green*) of the neighboring subunit, (b) the bottom of S4 to stay near the bottom of the pore domain at its own subunit end, and (c) maximal contact between S4 and the gating-sensitive residues on the surface of the pore domain. As can be seen, the model on the *left* makes the most S4 contacts with the gating-sensitive residues of the pore domain.

wash, it was possible to measure the rates of modification at negative potentials by washing the reagent off and allowing the channel to recover from inactivation between successive applications. Fig. 4*B* shows that the Cu-Phe-induced oxidation of the mutant channel occurred very rapidly at negative potentials with a time constant, τ, of 2.5 ± 0.2 min. The effects of the reagents on the open state of the channel could not be examined because of the rapid C-type inactivation (τ = 110.7 ± 13.1 ms) of the double mutant channel.

Interaction between Cys-357 and Cys-418 Occurs between the Subunits—We next asked whether Cys-357 lies in close proximity to Cys-418 from the same subunit or from one of the other subunits of the tetramer. To test this, we co-injected cRNA for the single mutant channels in a 1:1 ratio and recorded currents (Fig. 5). C-type inactivation (at 40 mV) measured from these currents (τ = 200.8 ± 27.8 ms) was intermediate between the corresponding single mutant channels (τ = 82.9 ± 1.8 ms for E418C; 2015.8 ± 84.1 ms for S357C), indicating that both mutant subunits were expressed. Application of Cd^{2+} caused a significant reduction (38.7 ± 7.6%) in the conductance of the channels expressed in the co-injected oocytes (Fig. 5*A*). The fact that Cd^{2+} did not affect the single mutant channels (Fig. 2) but inhibited currents through the co-expressed channels not only indicates that heteromers are formed but, more importantly, suggests the formation of metal bridges between the subunits, rather than within the subunits. The currents from co-injected oocytes were reduced by ~40% compared with that obtained from the double mutant channels. The magnitude of this inhibition corresponds to the theoretical inhibition of 37.5%, calculated with the assumption that only heteromers comprising two of each of the single mutant subunits are prone to inhibition by Cd^{2+}.

Voltage dependence experiments on the S357C/E418C (where the two mutants were co-expressed) heteromeric channel revealed that the application of Cd^{2+} at the hyperpolarized potential of −80 mV caused inhibition of currents (~25%) that could be slowly washed off during subsequent depolarizing pulses (Fig. 5*B*, *left*). No such inhibition was seen in controls where Cd^{2+} was omitted (Fig. 5*B*, *right*). Similar experiments with the Cu-Phe reagent resulted in ~14% inhibition at the hyperpolarized potential of −120 mV (Fig. 5*C*). These data demonstrate that position 357 of one subunit is close to position 418 of a neighboring subunit in the closed state of the channel.

DISCUSSION

In this study, we have investigated the possibility that the voltage-sensing S4 segment lies in close proximity to the perimeter of the pore domain at the extracellular end of the Shaker potassium channel. We demonstrate that cysteines introduced at positions 357 of S4 and 418 of the pore domain are close enough to be cross-linked with Cd^{2+} ions as well as disulfide bridges. The Cd^{2+} metal bridge appears to be formed between Cys-418 of one subunit and Cys-357 of a different subunit. We interpret these results to suggest that in the native channel, position 357 of S4 is close to position 418 of the pore domain of the neighboring subunit. Because these residues are located in the gating-sensitive regions of the channel protein, we propose that functional coupling of the voltage sensor to channel gating might occur through physical interaction between S4 and the pore domain.

Previous studies have shown that the S4 segment moves out of the transmembrane field in response to depolarization. This movement is somehow coupled to the opening of the activation gate formed by the crossing of S6 helices at the intracellular end of the pore. When activated, these helices may bend and splay open at a "gating hinge," thereby creating a wide entryway (12 Å) (9). In addition to the gating hinge, all K_v channels contain another flexible region, made up of Pro-X-Pro (unique

to voltage-gated channels), which is thought to make a bend during channel activation in order to direct the bottom of these helices toward the voltage sensor, thereby coupling the voltage sensor to the activation gates (2, 10, 11). Current evidence suggests that the motion of S4 is coupled to movement of the activation gate via the S4-S5 linker (43, 44). Although these studies are consistent with the presence of gating-sensitive residues near the intracellular entryway of the pore, MacKinnon and Yifrach (38) also reported the presence of a cluster of gating-sensitive residues near the extracellular end of the pore, implying potential interaction between S4 and the extracellular end of the pore domain. Consistent with this, there is some indirect evidence to suggest that S4 moves toward the extracellular end of the pore domain during depolarization (6, 29), although details of residue-residue contacts between S4 and the pore domain and how they move relative to each other during gating have not yet been determined. Kv channels also appear to contain a second activation gate in the selectivity filter (45) that may also be coupled to the movement of S4.

Here we found that Cd^{2+} inhibits the S357C,E418C double mutant Shaker channel but had no significant effect on the corresponding single mutant channels (Fig. 2), indicating that cysteines at these two positions contribute to the Cd^{2+} binding site and, hence, are close to each other. The inhibition is presumably caused by the restriction of the structural rearrangements necessary for channel activation. The inhibition occurred with an EC_{50} of 0.8 ± 0.1 μM, which is well within the concentration range previously shown to require participation of at least two liganding residues (12, 31, 33, 46). Additional evidence in support of the proximity of the residues at these two positions comes from the finding that Cu-Phe, a catalyst that promotes oxidation (34), was able to induce disulfide bridges between Cys-357 and -418 (Fig. 3*A*). This, together with the fact that ambient oxygen alone is sufficient to induce disulfide bridges (Fig. 3*B*), strongly supports the argument that positions 357 and 418 are close to each other in the three-dimensional structure of the channel. The propensity of the two cysteines to readily form a disulfide bridge suggests that the distance between the β-carbons in the disulfide-bonded cysteines may be close to 4.6 Å (24, 31, 34, 35). However, distance estimates obtained from the engineered disulfide approach tend to be less accurate because a number of factors can influence the rate of disulfide bridge formation. For example, thermal motions in a protein can bring cysteines as far apart as 15 Å close enough to result in a disulfide bridge, although this occurs very slowly (34). By contrast, Cd^{2+} has a relatively strict distance requirement, ~5 Å, for co-ordination to liganding residues (47). Both the Cd^{2+} binding and oxidation to disulfide bridges occurred in the closed state of the channel (Fig. 4). Thus, we conclude that in the closed state of the Shaker channel, positions 357 and 418 lie in close proximity (within ~5 Å) of each other. The data also suggest that the side chain of Cys-418 is most probably oriented toward the S4 helix in the closed state of the channel. In KcsA, the side chain of the corresponding residue, Glu-51, points into the core of the pore domain. However, as pointed out by Roux (37), it is possible that the structure of the turret in the Shaker channel, where Glu-418 is located, might be slightly different from that of KcsA.

The Cd^{2+} inhibition data were obtained from channels containing both S357C and E418C mutations within the same subunit. Because the Shaker channel is a tetramer, the interactions between 357 and 418 could be within a single subunit or between two subunits. The finding that Cd^{2+} reduced currents through heteromers composed of subunits bearing either S357C or E418C single mutations (Fig. 5) suggests that position 357 of one subunit is close to 418 of a neighboring subunit, most probably the adjacent one rather than the diagonal one. This may appear to contradict the current structural models (48) but would explain the gating perturbation studies by Swartz and co-workers (25), according to which the interface between the pore domain and the voltage-sensing domain is at a steep angle, located in a such a way that the extracellular end of this interface lies to one side of the subunit interface and the intracellular end at the other. Taken together with the findings of Swartz and co-workers (25), we propose that S4 lies at a steep angle relative to the pore axis, with the N-terminal end closer to the top of S5 of the neighboring subunit than its own (Fig. 6). Such a disposition would also be consistent with both the current models of S4 motion, *i.e.* S4 could move out of the transmembrane field by vertical translation and rotation (23) or by a motion involving twisting and tilting of S4 against another transmembrane segment such as S2 or S3 (1, 3, 22). Intriguingly, the disposition of S4 is equally compatible with other potential models, such as the relative lateral movement of crossed helices or a rocking motion at the interface between two domains, as has been proposed by Yellen (2).

In summary, our data demonstrate that residues situated just outside the membrane border of S4 (357) and S5 (418) of the Shaker channel lie in close proximity in the closed state of the channel. More importantly, our data indicate that the N-terminal end of S4 lies close to the C-terminal end of S5 of the neighboring subunit, suggesting that S4 might lie at a steep angle to the pore domain. We believe these findings will provide a new and important constraint for future molecular models of gating in voltage-gated ion channels and for subsequent verification of these models using appropriate experimental approaches such as those described in this study and elsewhere (12, 22, 23, 30).

Acknowledgment—We thank Dr. D. Donnelly for helpful discussions.

REFERENCES

1. Bezanilla, F. (2000) *Physiol. Rev.* **80,** 555–592
2. Yellen, G. (2002) *Nature* **419,** 35–42
3. Yellen, G. (1998) *Q. Rev. Biophys.* **31,** 239–295
4. Hille, B. (2001) *Ion Channels of Excitable Membranes*, 3rd Ed., Sinauer Associates, Inc. Sunderland, MA
5. Sigworth, F. J. (1994) *Q. Rev. Biophys.* **27,** 1–40
6. Loots, E., and Isacoff, E. Y. (2000) *J. Gen. Physiol.* **116,** 623–636
7. Doyle, D. A., Morais, C. J., Pfuetzner, R. A., Kuo, A., Gulbis, J. M., Cohen, S. L., Chait, B. T., and MacKinnon, R. (1998) *Science* **280,** 69–77
8. Zhou, Y., Morais-Cabral, J. H., Kaufman, A., and MacKinnon, R. (2001) *Nature* **414,** 43–48
9. Jiang, Y., Lee, A., Chen, J., Cadene, M., Chait, B. T., and MacKinnon, R. (2002) *Nature* **417,** 523–526
10. del Camino, D., Holmgren, M., Liu, Y., and Yellen, G. (2000) *Nature* **403,** 321–325
11. del Camino, D., and Yellen, G. (2001) *Neuron* **32,** 649–656
12. Liu, Y., Jurman, M. E., and Yellen, G. (1996) *Neuron* **16,** 859–867
13. Larsson, H. P., and Elinder, F. (2000) *Neuron* **27,** 573–583
14. Olcese, R., Latorre, R., Toro, L., Bezanilla, F., and Stefani, E. (1997) *J. Gen. Physiol.* **110,** 579–589
15. Kiss, L., and Korn, S. J. (1998) *Biophys. J.* **74,** 1840–1849
16. Baker, O. S., Larsson, H. P., Mannuzzu, L. M., and Isacoff, E. Y. (1998) *Neuron* **20,** 1283–1294
17. Larsson, H. P., Baker, O. S., Dhillon, D. S., and Isacoff, E. Y. (1996) *Neuron* **16,** 387–397
18. Wang, M. H., Yusaf, S. P., Elliott, D. J., Wray, D., and Sivaprasadarao, A. (1999) *J. Physiol.* **521,** 315–326
19. Yusaf, S. P., Wray, D., and Sivaprasadarao, A. (1996) *Pflugers Arch.* **433,** 91–97
20. Starace, D. M., Stefani, E., and Bezanilla, F. (1997) *Neuron* **19,** 1319–1327
21. Starace, D. M., and Bezanilla, F. (2001) *J. Gen. Physiol.* **117,** 469–490
22. Cha, A., Snyder, G. E., Selvin, P. R., and Bezanilla, F. (1999) *Nature* **402,** 809–813
23. Glauner, K. S., Mannuzzu, L. M., Gandhi, C. S., and Isacoff, E. Y. (1999) *Nature* **402,** 813–817
24. Aziz, Q. H., Partridge, C. J., Munsey, T. S., and Sivaprasadarao, A. (2002) *J. Biol. Chem.* **277,** 42719–42725
25. Li-Smerin, Y., Hackos, D. H., and Swartz, K. J. (2000) *Neuron* **25,** 411–423
26. Li-Smerin, Y., Hackos, D. H., and Swartz, K. J. (2000) *J. Gen. Physiol.* **115,** 33–50

27. Monks, S. A., Needleman, D. J., and Miller, C. (1999) *J. Gen. Physiol.* **113,** 415–423
28. Blaustein, R. O., Cole, P. A., Williams, C., and Miller, C. (2000) *Nat. Struct. Biol.* **7,** 309–311
29. Elinder, F., Mannikko, R., and Larsson, H. P. (2001) *J. Gen. Physiol.* **118,** 1–10
30. Liu, Y., Holmgren, M., Jurman, M. E., and Yellen, G. (1997) *Neuron* **19,** 175–184
31. Krovetz, H. S., VanDongen, H. M., and VanDongen, A. M. (1997) *Biophys. J.* **72,** 117–126
32. Tiwari-Woodruff, S. K., Lin, M. A., Schulteis, C. T., and Papazian, D. M. (2000) *J. Gen. Physiol.* **115,** 123–138
33. Tapper, A. R., and George, A. L., Jr. (2001) *J. Biol. Chem.* **276,** 38249–38254
34. Careaga, C. L., and Falke, J. J. (1992) *Biophys. J.* **62,** 209–216
35. Flynn, G. E., and Zagotta, W. N. (2001) *Neuron* **30,** 689–698
36. Farrens, D. L., Altenbach, C., Yang, K., Hubbell, W. L., and Khorana, H. G. (1996) *Science* **274,** 768–770
37. Roux, B. (2002) in *Ion Channels: From Atomic Resolution Physiology to Functional Genomics* (Block, G., ed) pp. 84–101, Novartis Foundation Symposium 245, John Wiley and Sons, Chichester, UK
38. Yifrach, O., and MacKinnon, R. (2002) *Cell* **111,** 231–239
39. Hoshi, T., Zagotta, W. N., and Aldrich, R. W. (1990) *Science* **250,** 533–538
40. Singh, R., Lamoureux, G. V., Lees, W. J., and Whitesides, G. M. (1995) *Methods Enzymol.* **251,** 167–173
41. Ruegg, U. T., and Rudinger, J. (1977) *Methods Enzymol.* **47,** 111–116
42. O'Sullivan, W. J. (1969) in *Data for Biochemical Research* (Dawson, R. M. C., Elliott, D. C., Elliott, W. H., and Jones, K. M., eds) Oxford University Press, Oxford
43. Lu, Z., Klem, A. M., and Ramu, Y. (2002) *J. Gen. Physiol.* **120,** 663–676
44. Hackos, D. H., Chang, T. H., and Swartz, K. J. (2002) *J. Gen. Physiol.* **119,** 521–532
45. Zheng, J., and Sigworth, F. J. (1997) *J. Gen. Physiol.* **110,** 101–117
46. Loland, C. J., Norregaard, L., and Gether, U. (1999) *J. Biol. Chem.* **274,** 36928–36934
47. Rulisek, L., and Vondrasek, J. (1998) *J. Inorg. Biochem.* **71,** 115–127
48. Durell, S. R., Hao, Y., and Guy, H. R. (1998) *J. Struct. Biol.* **121,** 263–284